ISIJ International, Vol. 33 (1993), No. 1, pp. 166–175

Observations on the Role of Interfacial Phenomena in Materials Processing

B. S. TERRY and P. GRIEVESON

Department of Materials, Imperial College, London SW7, UK.

(*Received on June 8, 1992; accepted in final form on September 18, 1992*)

Examples of the role interfacial phenomena can play in materials processing are highlighted in the description of a number of recent research studies conducted at Imperial College. Interfacial phenomena play critical roles in increasing or retarding the rates of chemical reaction and in promoting or hindering wetting and dispersion of phases in each other.

The reduction of ilmentite to iron and titanium carbide or titanium oxycarbide has been studied with the ultimate aim of achieving separation of the titanium and its subsequent conversion to pigment grade titanium dioxide. The need to achieve good separation of iron from other reaction products is then a prime concern. The effects of reducing conditions on the wetting of titanium carbides and oxycarbides by iron alloys has therefore been studied. It seems that associative adsorption of titanium and carbon may be responsible for the observed effects of dissolved titanium and carbon on the wetting of TiC by liquid iron alloys.

As a result of this work a further project has been generated involving the identification of conditions for achieving good dispersions of refractory carbides including titanium carbide in iron alloys. The major motivation behind this work was the desire to develop a cheap casting based process for the production of iron based metal matrix composites capable of producing near net shape products. As a result of this work a novel rapid testing technique for the assessment of the wettability and compatibility of potential filler materials with liquid metal matrices has been developed. The technique employs levitation and quenching of liquid metal drops containing added filler materials to permit assessment of alloy composition, filler coatings and temperature on matrix/filler interactions. The levitation technique has been further utilised in a study of the conditions required for dispersion or non dispersion of second phase particles in liquid superalloys. In this case the cleanliness of the superalloys achieved during recyling procedures is determined by the ease with which inclusions can be removed. Some observations with ternary oxides also indicate the importance of the associative adsorption phenomenon.

The importance of interfacial considerations has also been highlighted by our studies on the production of aluminium–titanium–boron grain refining master alloys from fluoride fluxes. Entrapment of the products can result from emulsification occurring during the reduction reactions. A detailed study of this phenomenon has been conducted using a modified sessile drop technique. The results obtained indicate the critical role that interfacial tension plays in determining the ease of metal–flux separations and in determining whether products are dispersed in the metal or slag.

The kinetics of metal–salt reactions were also found to be of importance. Fast transfer of Ti and B to the metal results in the build up to $TiAl_3$. TiB_2 or AlB_{12} at the interface. These compounds when present at the interface can be wet by the flux and result in emulsion formation. Inhibition of emulsification can be achieved by the presence of surface active elements such as magnesium and calcium.

The role of interfacial phenomena in influencing the kinetics of the reduction of slags has been studied in an investigation of the kinetics of alkali metal oxide release from silicate melts. The kinetics of K_2O and Na_2O release during heating in graphite crucibles has been studied from binary alkali oxide–silicon dioxide melts and from a wide range of CaO–Al_2O_3–SiO_2 slags. The contribution of the wetting of the graphite by the slag towards influencing reaction kinetics represents a notable feature of the study.

KEY WORDS: interfacial phenomena; materials processing.

1. Introduction

This paper seeks to highlight examples of the role interfacial phenomena can play in materials processing by describing a number of recent research studies conducted at Imperial College. Interfacial phenomena play critical roles in increasing or retarding the rates of chemical reaction and in promoting or hindering wetting and dispersion of phases in each other. Surface active species when present even in very small quantities can markedly alter interfacial properties with resulting effects on chemical reactions and dispersion of phases. Such effects are clearly therefore of great importance in both the development of novel production and processing

routes and in understanding and optimising existing routes.

2. Reduction Carburisation of Ilmenite

The reduction-carburisation of ilmenite (nominally $FeTiO_3$) to iron and titanium carbide or titanium oxycarbide has been studied[1,2] with the ultimate aim of achieving separation of the titanium content and its subsequent conversion to pigment grade TiO_2.

A considerable volume of research work has been devoted by many workers to the reduction of ilmenite to produce oxide and iron. In all cases physical separation of the oxide proved difficult. The need to achieve good separation of iron from other reaction products is a prime concern and with this in mind it was felt by us that production of a carbide rather than an oxide phase might prove beneficial. We have, therefore, conducted a detailed study of the effect of reducing conditions on the mechanism of the carbothermic reduction of ilmenite by considering kinetic data and microstructural examination and X-ray diffraction of reaction products. Full details of experimental techniques and conditions employed and the results obtained are provided elsewhere.[1,2]

Table 1. X-ray diffraction analyses of WMS ilmenite reduced at 1 314°C using 'collie' coal.

Time of reaction	% Reaction	Phases present
7 min	24	M_3O_5, Fe, TiO_xC_y (trace)
17 min	42	M_3O_5, Fe, TiO_xC_y
30 min	52	M_3O_5, Fe, TiO_xC_y
65 min	65	Fe, TiO_xC_y
120 min	77	Fe, TiO_xC_y
154 min	82	Fe, TiO_xC_y

Table 2. X-ray diffraction analysis of phases produced at 1 413°C.

Reaction time	% Reaction	Phases present
18 min	50%	Ti_3O_5, Ti_2O_3, Fe, TiO_xC_y; $a=4.296$ Å
45 min	55%	Ti_2O_3, Fe, TiO_xC_y; $a=4.293$ Å
63 min	66.5%	Ti_2O_3, TiO_xC_y; (2*a*) $a=4.285$ Å, $a=4.303$ Å, Fe
180 min	75.7%	Ti_2O_3, TiO_xC_y; (2*a*) $a=4.289$ Å, $a=4.300$ Å, Fe

(2*a*) Two diffraction patterns.

Table 3. X-ray diffraction analysis of WMS ilmenite reduced with 'collie' coal at 1 517°C.

Reaction time	% Reaction	Phases Present
5 min	62	M_2O_3, TiO_xC_y; $a=4.300$ Å, Fe, M_3O_5 (trace)
30 min	87	M_2O_3, TiO_xC_y; $a=4.302$ Å, Fe
45 min	93	M_2O_3, TiO_xC_y; $a=4.305$ Å, Fe, Fe_3C (trace)

2.1. Reduction Products

The experimental evidence obtained from X-ray diffraction analysis (**Tables 1–3**) clearly shows that titanium oxycarbide can be formed from both Ti_3O_5 and Ti_2O_3 produced by the reduction of ilmenite. At 1314°C conclusive evidence has been produced to show that the oxycarbide forms from Ti_3O_5. At 1 517°C on the other hand evidence has been produced to show that the oxycarbide forms from Ti_2O_3. At 1413°C our results indicate that the conditions for formation of oxycarbide from ilmenite are closely balanced for production from Ti_2O_3 and Ti_3O_5. It was, therefore, concluded that at temperatures below 1 413°C oxycarbide forms from Ti_3O_5 in contact with iron whilst at higher temperatures it forms from Ti_2O_3. A progressive increase in the carbon content and associated decrease in the oxygen content

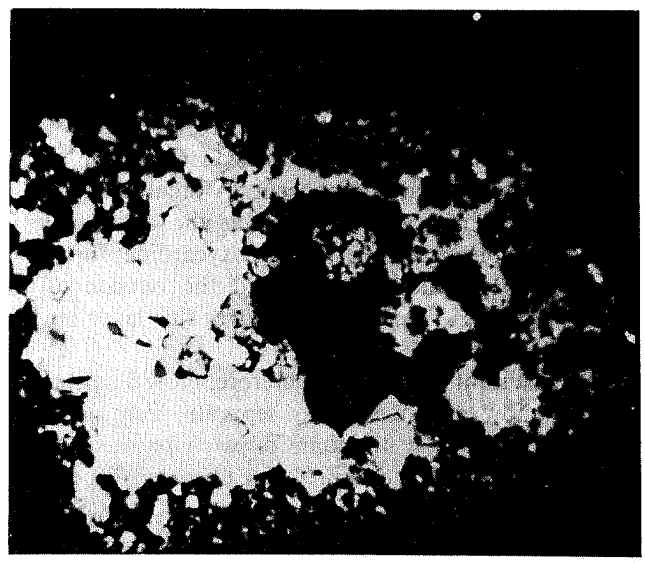

Fig. 1. 1 h reduction.

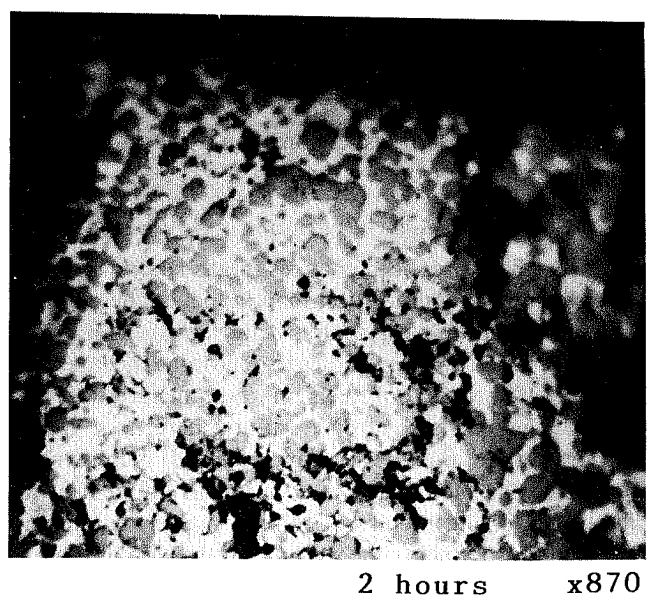

Fig. 2. WMS ilmenite+coal 1 314°C. White phase: iron light grey: titarium oxycarbide; dark grey; M_3O_5.

of the oxycarbide phase was observed with increasing reduction temperature.

For reduction at 1 314°C micrographic examination showed that in the initial stages of reduction Ti(O, C) existed as a separate phase between iron and Ti_3O_5 with clear separation from the iron phase as shown in **Fig. 1**. However, as the reaction proceeded the oxycarbide phase became dispersed in the molten iron as shown in **Fig. 2**. This suggests that the initial phase separation of iron occurs from titanium oxides at which time oxycarbide forms. The oxycarbide is initially separated from the iron and then gradually becomes dispersed in the molten iron phase. A similar development of product microstructure was observed during reduction at 1 413°C except that the reaction occurred more rapidly. Thus a fine oxycarbide phase was formed completely dispersed in molten iron after 4 h. Subsequent heat treatment caused the oxycarbide particles to coarsen due to Ostwald ripening producing larger oxycarbide particles dispersed in the molten iron.

Optical microscopic examination of the reaction products of reduction at 1 517°C revealed several differences in structure from the lower temperature reduction products in which Ti(O, C) formed from Ti_3O_5. After 5 min iron and Ti_2O_3 formed and separation of the two phases started to occur. A small quantity of oxycarbide phase was observed at the outer edge of the oxide phase. After 10 min oxycarbide formed a continuous product layer around the outside of the titanium oxide. The iron spread over this layer but did not penetrate it.

The results of our studies, therefore, show that titanium oxides show a tendency to separate from the iron produced and that titanium oxycarbide was initially separated but as reaction proceeded became dispersed in the liquid iron. These results agree to some extent with those of O'Brien and coworkers[3-5] who have reported that titanium oxycarbide formation inhibits the separation of iron from titanium oxides. It also appears that Ti_2O_3 shows a greater tendency to disperse in molten iron than does Ti_3O_5.

3. Conditions for Dispersion

The conditions for dispersion of an oxide or oxycarbide phase in molten iron are that

$$\sigma_{Ti-O-C} > \sigma_{gas/Fe} + \sigma_{Fe/Ti-O-C} \quad \text{or} \quad (\sigma_{Fe/Tioxide})$$

Clearly, therefore, both changes in gas composition and in molten iron composition may influence the degree of dispersion obtained. Kiparisov and coworkers[6,7] have performed sessile drop studies to determine the interfacial tension of various tool steels on titanium carbide. It was found that in a hydrogen atmosphere less wetting occurred than in an argon atmosphere. It is known that oxygen is surface active in solution in liquid iron and hydrogen could, therefore, be responsible for removing oxygen thus reducing the wetting. In the case of titanium carbide, this explanation is not sufficient as it is known that titanium oxides separate from liquid iron so any reduction would be enhance wetting. Hydrogen is also likely to cause decarburisation of liquid iron. Although carbon is known to have little effect on the surface tension of liquid iron, there is evidence that in the presence of carbide forming elements such as silicon and chromium, it has a considerable effect.[8] Belton[9] presented an analysis of work carried out on the effect of chromium and carbon on the surface tension of liquid iron and proposed that a surface active "compound" CrC was formed. It seems reasonable to suggest that titanium and carbon will behave in a similar manner thus causing a reduction in the surface tension of liquid iron as the titanium and carbon content increases. Such an effect would explain the observations of a reduction in wetting of TiC in a hydrogen atmosphere as a result of decarburisation of the iron.

Our observation on the reduction of ilmenite can also be largely explained by this hypothesis of associative adsorption of titanium and carbon. As reduction of ilmenite takes place dissolution of titanium and carbon in the molten iron product will also occur eventually permitting wetting of the titanium oxycarbide formed and hence producing its observed redispersion.

Further support for this hypothesis was gained by our observations[2] that a decarburisation treatment of pre-reduced ilmenite permits separation of globules of metallic iron.

3.1. Production of Fe–TiC Composites

The observed dispersion of oxycarbide in iron during the reduction of ilmenite defeated one of our major objectives *i.e.* easy separation of iron from the titanium bearing constituent. However, the condition of dispersion of refractory materials in liquid metals of prime interest in the production of wear resistant composite materials. We have, therefore, extended our ilmenite reduction work with a view to producing good dispersions of TiC and/or Ti(OC) in iron bearing matrices.[10] On a laboratory scale, we have achieved notable success in obtaining excellent dispersions of Ti(O, C) in iron matrices by the direct reduction of ilmenite and rutile in the presence of iron. As part of this study, we have developed a simple levitation test[11] for assessing the dissolution and dispersion of ceramic particles in molten metals. The technique employs levitation and quenching of liquid metal drops containing added filer materials to permit assessment of alloy composition, filler coatings and temperature on marix/filler interactions. The major motivation behind this work was the desire to develop a cheap casting route for the production of iron based composites. Results obtained from this test indicate that titanium carbide is more readily dispersed than titanium oxycarbide and that titanium oxycarbide produced *in situ* in molten iron is more readily dispersed than titanium oxycarbide produced by a separate process. The results also show that dispersion is strongly favoured by high contents of dissolved titanium and carbon in the molten iron. Once again these results appear to be in agreement with our hypothesis of associative adsorption of titanium and carbon. The results also indicate the merit of producing ceramic additions *in situ* and thus avoiding detrimental effects of surface oxides with respect to

dispersion.

We are about to commence a more detailed study of the effects of binary additions of solutes to molten iron on the surface tension of iron and the dispersion of second phases with a view to identifying conditions where associative adsorption operates. We have also extended our assessment of dispersion and reaction of second phase particles in molten iron to study the behaviour of SiC,[12] B_4C[13] and TiB_2[14] once again with a view to developing processing routes for the production of wear resistant composites.

3.2. Dispersion of Second Phase Particles in Liquid Superalloys

The levitation technique we have developed for assessing the dispersion of second phase particles in molten metals is also applicable to the study of factors influencing inclusion removal. We have utilised the technique in a study of conditions required for dispersion or non-dispersion of second phase particles in liquid superalloys.[15] In this case the cleanliness of the superalloys achieved during recycling procedures is determined by the ease with which inclusions can be removed.

As part of the study wetting characteristics of liquid nickel, with ceramic particles have been assessed. A notable finding is that whilst binary oxides such as MgO and Al_2O_3 were found to be non wetting on their own when present together as the aluminate $MgAl_2O_4$ they were found to be wetted by the nickel melts. This is indicative of some form of cooperative or associative effect occurring at the interface. Similar effects have been observed in systems such as NiO/Al_2O_3, CaO/Al_2O_3 and MnO/Al_2O_3. This ability to form aluminates which are wet by liquid nickel poses significant problems with the removal of inclusions from melts held in magnesia or calcia crucibles.

4. Production of Aluminium–Titanium–Boron Alloys

Al–Ti–B alloys are commonly used to impart grain refining in the casting of aluminium. They are produced by the reaction between molten aluminium and potassium fluorotitanate K_2TiF_6 and potassium fluoroborate KBF_4. Significant problems associated with this production route include entrapment of $KF–AlF_3$ flux product in the metal alloy product and agglomeration of TiB_2 particles in the alloy product. We have conducted a detailed study of interfacial phenomena related to these reactions and have reported our results in full elsewhere.[16,17]

The experimental procedure employed essentially involved a modified sessile drop technique in which

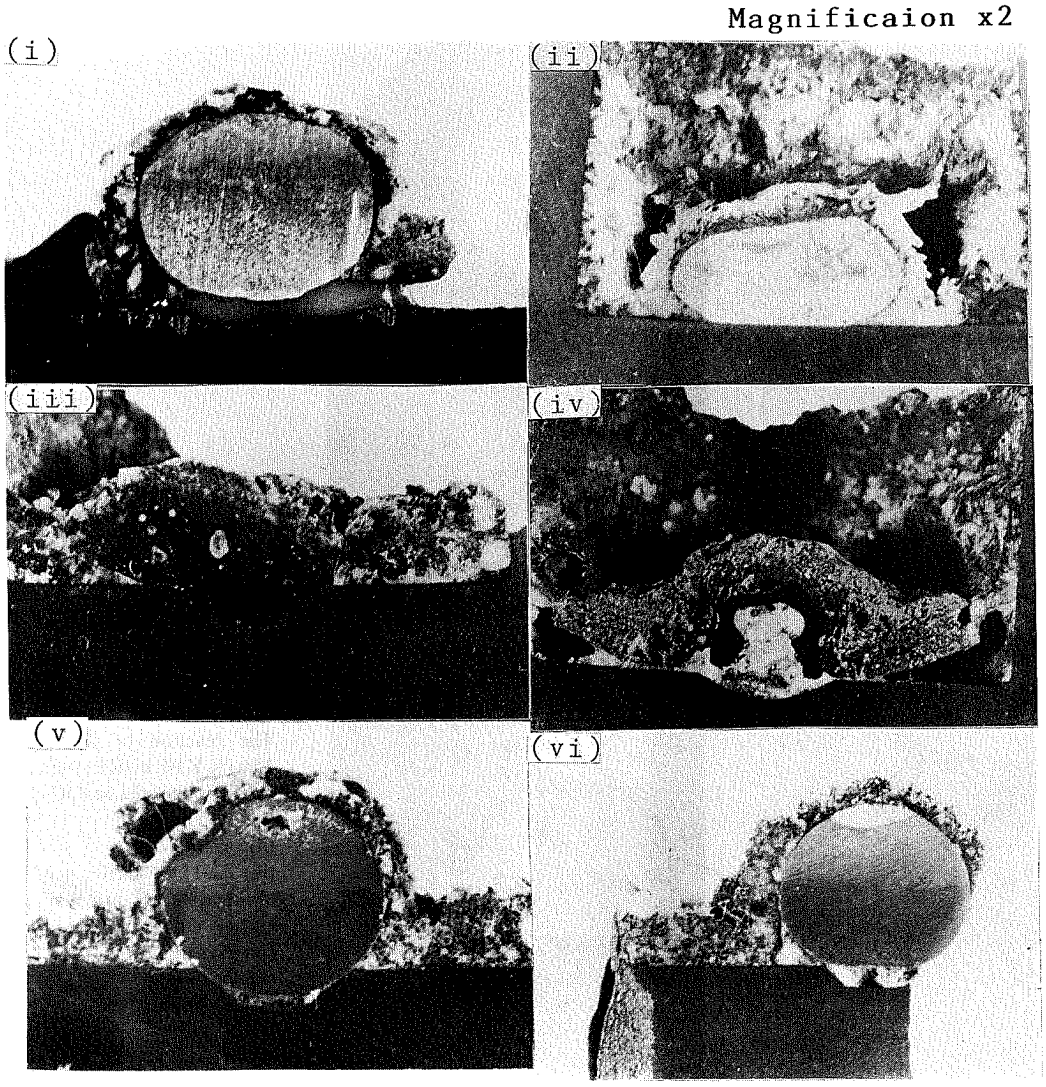

Fig. 3.
The reaction of Al with various flux composition for 15 min at 720°C.
(i) 2.7 wt% K_2TiF_6 in $(KF–AlF_3)_E$.
(ii) 7.5 wt% K_2TiF_6 in $(KF–AlF_3)_E$.
(iii) 9 wt% K_2TiF_6 in $(KF–AlF_3)_E$.
(iv) 12 wt% K_2TiF_6 in $(KF–AlF_3)_E$.
(v) 7.5 wt% K_2TiF_6 + 1 wt% CaF_2 in $(KF–AlF_3)_E$.
(vi) 7.5 wt% K_2TiF_6 + 1 wt% MgF_2 in $(KF–AlF_3)_E$.

molten aluminium alloy was contacted with an appropriate salt or flux composition in a graphite crucible. The crucible and its contents were then quenched to room temperature and sectioned to determine the shape of the metal drop. Experiments were conducted using an aluminium pellet contacted with a $KF–AlF_3$ flux of eutectic composition (45 mol% AlF_3, ss mol% KF) to which were added additions of K_2TiF_6 and/or KBF_4. Analogous experiments were conducted in corresponding sodium systems. Some of our most interesting observations are described below.

4.1. Al–Ti/KF–AlF_3

Figure 3 shows the results obtained by reacting various flux compositions with aluminium at 720°C. These results show a reduction in interfacial tension with increasing K_2TiF_6 level in the flux and hence with increasing resultant Ti level in the aluminium alloy product. At a critical K_2TiF_6, initial level in the flux a metal emulsion is formed as shown in Fig. 3(iv). At K_2TiF_6 concentrations in the flux lower than that the $TiAl_3$ produced by the aluminium/flux reaction is dispersed in the metal phase. Addition of Ca or Mg to the system was found to increase the interfacial tension and prevent emulsification as shown in Figs. 3(v) and 3(vi). Mg and Ca are known to be surface active in aluminium. It appears that Mg and Ca are effective in preventing emulsification by occupying surface sites in the aluminium and so inhibiting the Al–K_2TiF_6 reaction. The rate of formation of $TiAl_3$ is decreased and a build up of $TiAl_3$ at the surface which may cause metal–flux emulsification is prevented. Our results indicate that a certain critical level of Mg or Ca in the flux is required to prevent the $TiAl_3$ being dispersed in the flux. The level of Mg required to prevent emulsification is less than the corresponding calcium level. The level of Mg or Ca required increases with increasing reaction temperature.

4.2. Al–B/KF–AlF_3

AlB_{12} forms as a metastable phase during the reaction of $KF–AlF_3$ containing KBF_4 with liquid aluminium. The AlB_{12} phase can be dispersed in either the flux or metal phase depending on the process conditions. In this case magnesium and calcium additions are not effective in increasing interfacial tension and we have attributed this to the formation of magnesium and calcium hexaborides. **Figure 4** shows the results obtained when KBF_4 was added to Al under $KF–AlF_3$ flux at 740°C. The interfacial tension is seen to decrease initially (Fig. 4(i)), achieve minimum value (Figs. 4(ii) and 4(iv)) after 4 min of reaction and then beging to increase again after $7\frac{1}{2}$ min (Figs. 4(v) and 4(vi)).

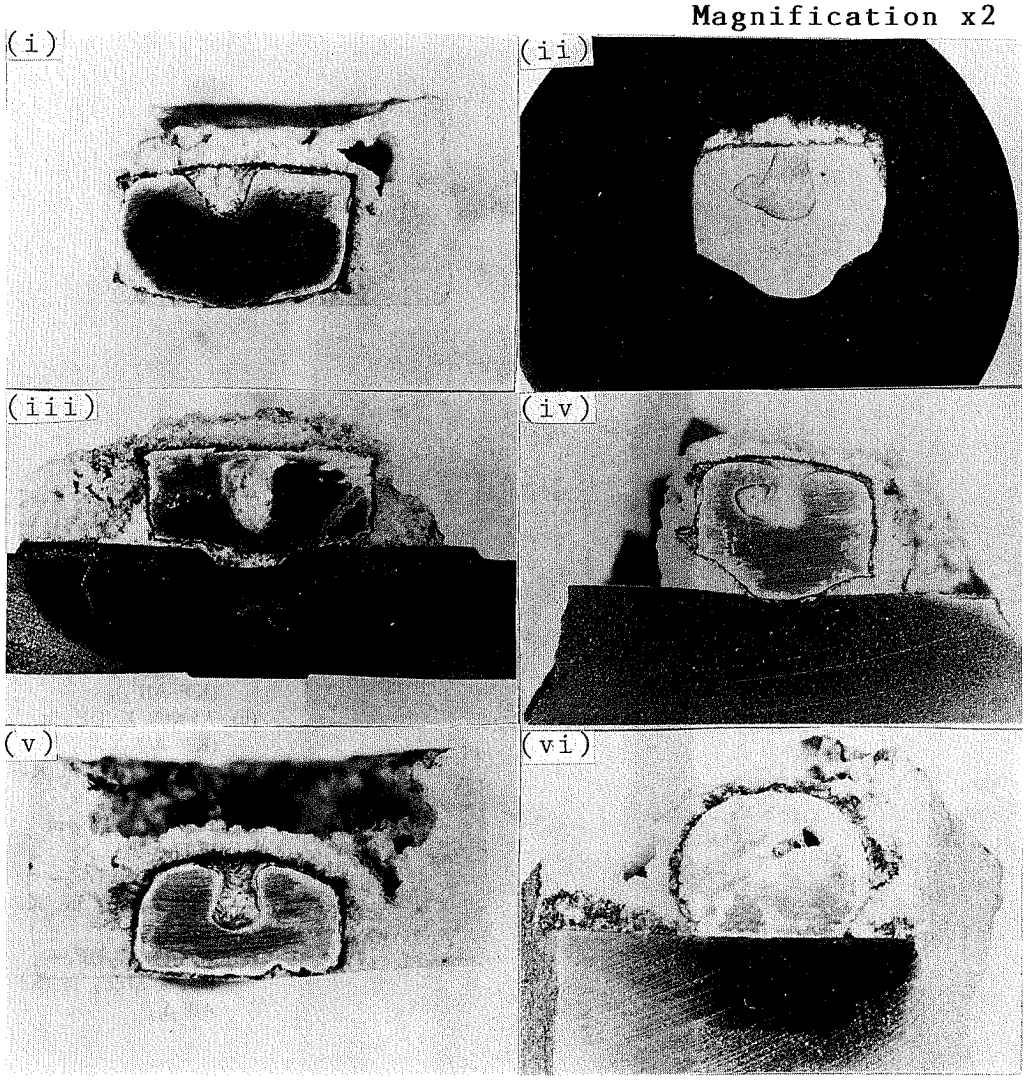

Fig. 4.
The reaction of Al with 15 wt% KBF in $(KF–AlF_3)_E$ for various times at 740°C.
(i) $t=1$ min.
(ii) 4 min.
(iii) Al–15 wt%KBF_4 + 1 wt%CaF_2 in $KAlF_4$; $t=4$ min.
(iv) $t=6$ min.
(v) $t=7\frac{1}{2}$ min.
(vi) $t=9$ min.

Such lowering and disappearance of interfacial process during the course of a reaction has previously been explained as a result of intense mass transfer at the interface.[18] Our observations indicate that reduction of KBF_4 by aluminium is likely to occur within the first 30 sec of reaction and this, therefore, should be the period of most intense mass transfer. The fact the the minimum in the interfacial tension is not achieved until several minutes after the most intense mass transfer has finished suggests the conventional explanation for the minimum in interfacial tension is questionable in this case.

4.3. Al–Ti–B/KF–AlF_3

Co-reduction of K_2TiF_6 and KBF_4 salts by aluminium in the presence of KF–AlF_3 flux produces TiB_2 particles that can be wet by either the flux or metal with high salt levels in the flux favouring wetting by the flux. Our findings indicate that it is this wetting by the flux during the initial stages of the commercial production of grain refining alloys that leads to the production of TiB_2 agglomerates in which the TiB_2 is held together by the flux. This flux effectively shields the TiB_2 particles from the aluminium melt and prevents their subsequent redispersion.

5. Kinetics of Alkali Metal Release from Slags

The role of interfacial phenomena in influencing the kinetics of reduction of slags has been studied in an investigation of the kinetics of alkali metal release from silicate melts. The kinetics of K_2O and Na_2O release during heating in graphite crucibles has been studied from binary alkalioxide–silica melts and from a wide range of CaO–Al_2O_3–SiO_2 slags. The overall aim of the work was to establish mechanism and kinetics of alkali release from slags relevant to blast furnace ironmaking and coal gasification and combustion processes.

Full details of the experimental procedures employed and the results obtained are reported elsewhere.[19–22]

Different compositions of these slags (SiO_2, Al_2O_3, CaO) were produced for coal gasifier type slags (C.G.S.) and blast furnace type slags (B.F.S.). The coal gasifier type slags contained a higher percentage of Al_2O_3 but a lower percentage of CaO than the blast furnace type slags.

Each master slag was heated to just above its melting point. The melting point of each master slag was estimated by calculating the molar fraction of each of the three oxides present and plotting them on their ternary phase diagram. The master slags were melted by a radio frequency generator in graphite crucibles inside a silica vessel under argon or CO_2 gas according to the stage of experiment for 2 h. These slags were then cooled down inside the vessel with the argon or CO_2 running until the temperature of approximately 200°C was achieved and were then finally air cooled to room temperature.

The master slags were removed from the crucibles with varying difficulty depending on whether they reacted with the crucible or not. The slags were then crushed into particles of approximately 3 mm in diameter with a pestal and mortar and then ground to fine powders inside a tema mill. Nominal additions of 4 or 7% alkali (K_2O or Na_2O) were made to each master slag in the form of carbonates (K_2CO_3 or Na_2CO_3). The slag and the alkali (either K_2CO_3 or Na_2CO_3) were finely mixed as powder before being heated at 1 450°C for 2 h under the same atmosphere and conditions as the master slags were prepared. They were then once again crushed and ground ready for chemical analysis.

Coal gasifier and blast furnace slags with alkali additions were heated for various times at various temperatures and were then analysed for potassium, sodium and silicon. The effects of varying gas atmosphere (CO, argon) gas flow rate, crucible size and stirring of the slag were studied. In addition the effects of using new or previously used crucibles and of employing a copper lined crucible were investigated.

Finally additions of CaS, FeS, Fe and graphite were made to the slags and the resultant effects on alkali release were determined. Alkali release from various compositions in the K_2O–SiO_2 and Na_2SiO_2 systems was also

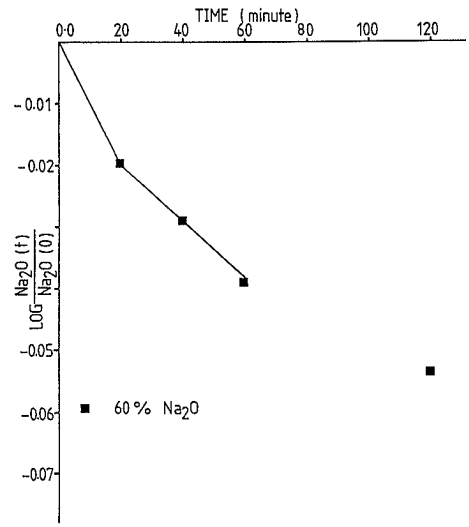

Fig. 5. Kinetics of Na_2O release from Na_2O–SiO_2 slags at 1 300°C.

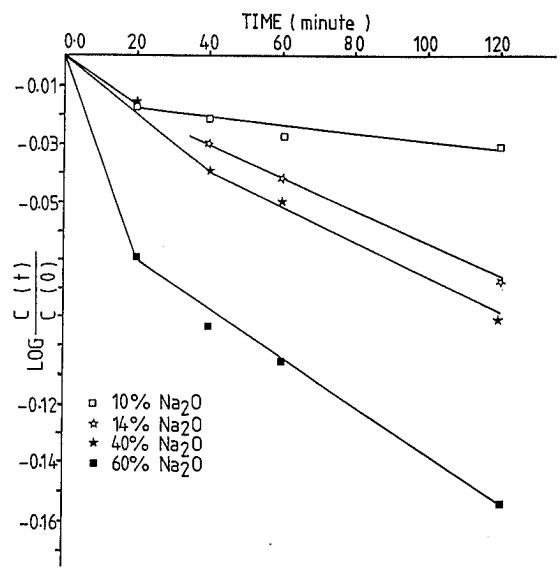

Fig. 6. Kinetics of Na_2O release from Na_2O–SiO_2 slags at 1 500°C.

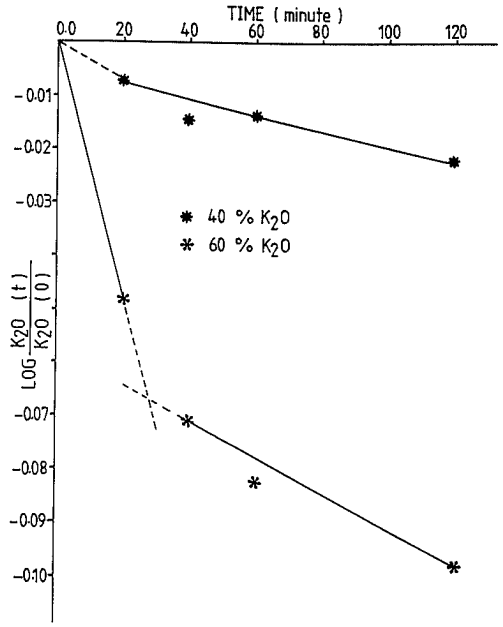

Fig. 7. Kinetics of K_2O release from K_2O–SiO_2 slags at 1 300°C.

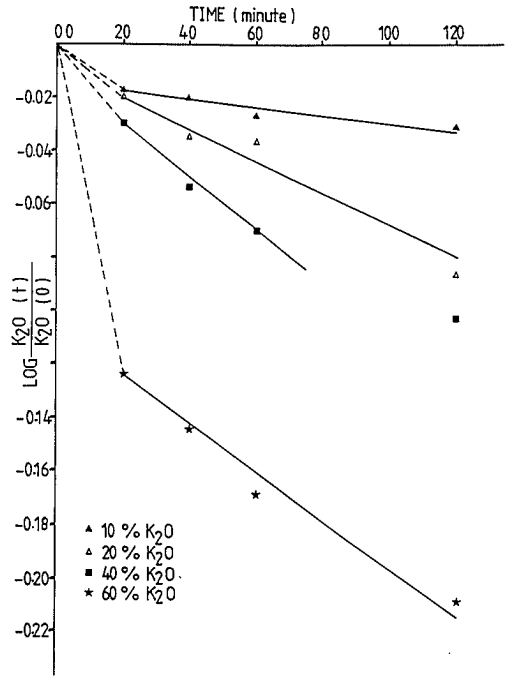

Fig. 8. Kinetics of K_2O release from K_2O–SiO_2 slags at 1 500°C.

investigated in a similar manner.

5.1. Alkali Relase from K_2SiO_2 and Na_2–SiO_2 Melts

Figures 5–8 show data obtained for the rate of Na_2O and K_2O release from Na_2O–SiO_2 and K_2O–SiO_2 slags plotted in the form of $\log(Na_2O(t)/Na_2O(0))$ and $\log(K_2O(t)/K_2O(0))$ *vs.* time. These figures clearly show the establishment of two distinct regions each showing an approximately linear relationship with time. The melts containing 60 % Na_2O or 60 % K_2O show a particularly fast initial stage whereas for other slag compositions the rate of the first stage is significantly slower and is much closer to that of the second stage. The data for the 60 % Na_2O and 60 % K_2O melts have been analysed assuming

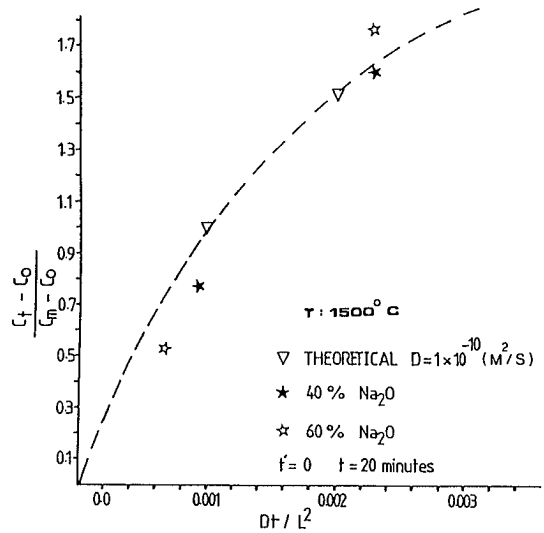

Fig. 9. Comparison of measured rates of Na_2O release from slags (Na_2O–SiO_2) and those assuming diffusion is rate controlling in slags.

Table 4. Comparison of estimates of D_{Na_2O} and D_{K_2O} with literature values.

Present study

Temperature (°C)	Initial % Na_2O	D_{Na_2O} ($m^2 s^{-1}$)
1 300	60	1.5×10^{-11}
1 500	10	4.0×10^{-11}
1 500	14	6.0×10^{-11}
1 500	40	1×10^{-11}
1 500	60	1×10^{-10}
Temperature (°C)	**Initial % K_2O**	**D_{K_2O} ($m^2 s^{-1}$)**
1 300	40	4×10^{-12}
1 300	60	1.4×10^{-11}
1 500	19	5×10^{-12}
1 500	20	9×10^{-11}
1 500	40	1×10^{-10}
1 500	60	9×10^{-11}

Literature values

Temperature (°C)	Composition	D_{Na_2O} ($m^2 s^{-1}$) (Ref. 27))
1 500	30%Na_2O–70%SiO_2	4.0×10^{-11}
1 500	40%Na_2O–60%SiO_2	2.3×10^{-11}
1 500	50%Na_2O–50%SiO_2	1×10^{-11}
Temperature (°C)	**Composition**	**D_{K_2O} ($m^2 s^{-1}$) (Ref. 28))**
1 300	30%K_2O–70%SiO_2	7.5×10^{-12}
1 500	30%K_2O–70%SiO_2	3.0×10^{-11}

mass transfer in the slag is rate controlling. The second stage results when gas bubble generation ceases and diffusion becomes the only means of transporting alkali oxide to the slag/gas interface.

Gas bubble generation is brought about by the following reactions:

$$K_2O + C = 2K_{(g)} + CO_{(g)} \quad \text{.....(1)}$$

$$SiO_2 + C = SiO_{(g)} + CO_{(g)} \quad \text{.....(2)}$$

$$Na_2O + C = 2Na_{(g)} + CO_{(g)} \quad \text{.....(3)}$$

At 1 500°C the observed change in mechanism occurs at a melt composition of 51%Na_2O–49%SiO_2 and at a melt composition 45%K_2O–55%SiO_2. Using the activity data of Rego *et al.*,[23] it can be shown that for the Na_2O melt the above composition will yield a total gas pressure of 3 atm according to Eq. (1). Similarly using the activity data of Steiler *et al.*,[24] it can be shown for the K_2O melt the above composition will yield a total gas pressure of 1.5 atm according to Eq. (3).

It can be readily shown that the SiO generating reaction (2) is not as important as the alkali generating reactions (1) and (3). In view of the likely accuracy of the activity data employed, it appears to be a reasonable assumption that the initially rapid kinetics of alkali release from 60 % K_2O, 40 % SiO_2 and 60 % Na_2O, 40 % SiO_2 slags ceases because there is no longer sufficient thermodynamic driving force to permit nucleation of gas bubbles within the melt. It is thought that in all the other melts studied the initial rapid rate of alkali release arose as a result of alkali release during preheating to the temperature of the experiment leading to a false high rate of alkali release in the initial stages of the experiments. All subsequent rates appear to be controlled by diffusion in the slag.

As all melts adopted a spherical shape covering the entire base of the crucible the diffusion process can be crudely approximated as being the same as diffusion to the surface of an hemisphere of the same radius as the graphite crucible employed. Figure 5 shows an example of theoretical predictions obtained by judicious choice of the diffusion coefficient of the alkali oxide diffusion coefficient, with experimental data for the Na_2O–SiO_2 system at 1 500°C. Considering the approximation made a good fit is obtained. Similar good fits were obtained for all melt compositions studied. **Table 4** lists the values of D required to achieve a good fit between theoretical prediction and experimental data and indicates a reasonable agreement with literature data.

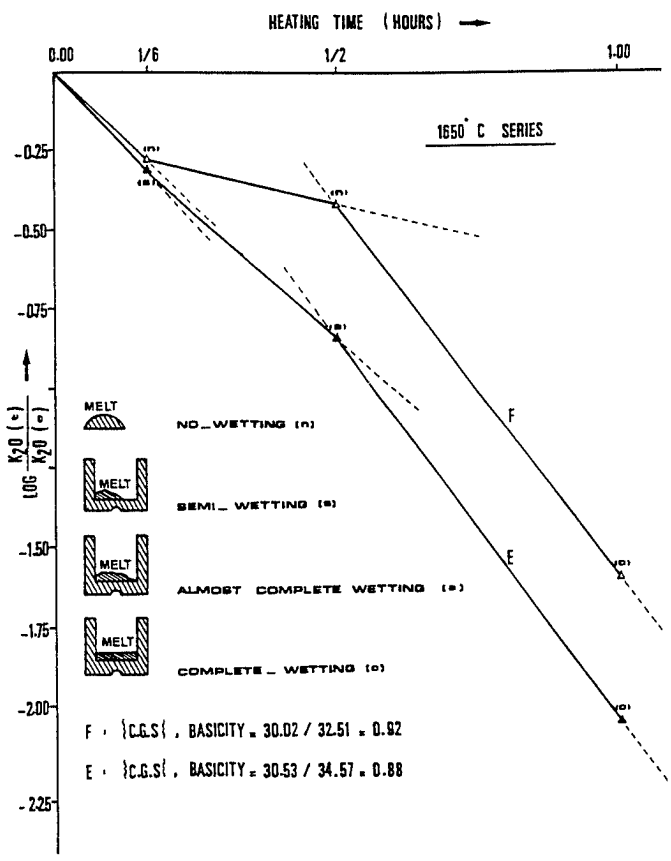

Fig. 10. K_2O release from CaO–Al_2O_3–SiO_2 slags at 1 650°C.

5.2. Alkali Release from CaO–Al_2O_3–SiO_2 Slags

Typical data obtained for the rate of alkali release from CaO–Al_2O_3–SiO_2 slags are shown in **Figs. 10** and **11**. Depending on conditions alkali release exhibits either 2 or 3 stages.

With the exception of runs where additions of graphite powder were deliberately made to the slags, stage 1 of the reduction kinetics was considerably short in duration. It seems likely, therefore, that the observed rapid reaction kinetics during this stage can be prescribed to alkali release occurring during preheating to the temperature of the experiment.

When graphite powder was added to slags, stage 1 kinetics corresponded to significantly larger losses of alkali. It is proposed that addition of graphite to the slags promotes CO bubble generation resulting in stirring and mass transfer control of kinetics. In the absence of graphite there is either insufficient carbon surface area or the graphite of the crucible is insufficiently reactive to provide sufficient CO bubble generation.

The following relationship has been established for liquid phase mass transfer resulting from stirring by gas bubbles[25]

$$k_m^2 = bDQ \quad \text{.....(4)}$$

where, k_m: mass transfer coefficient
b: constant
D: diffusivity
Q: volume flow of gas bubbles.

If it is assumed that the volume flow of gas bubbles generated as a result of graphite powder additons is

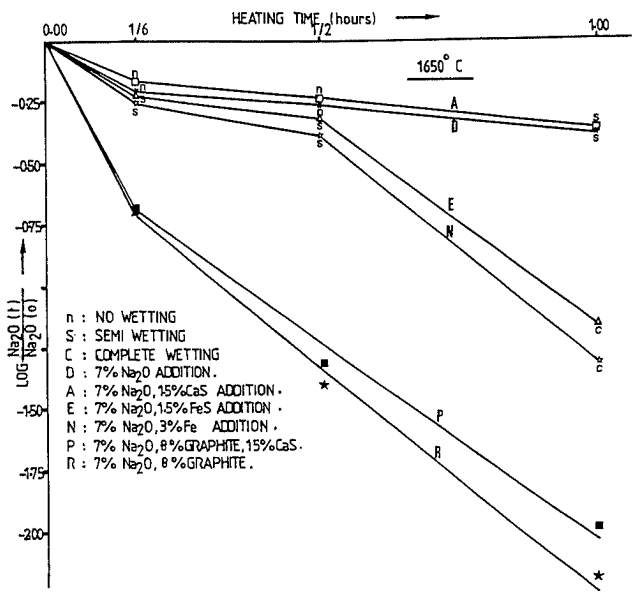

Fig. 11. Effect of iron, graphite and sulphur additions on Na_2O release at 1 650°C.

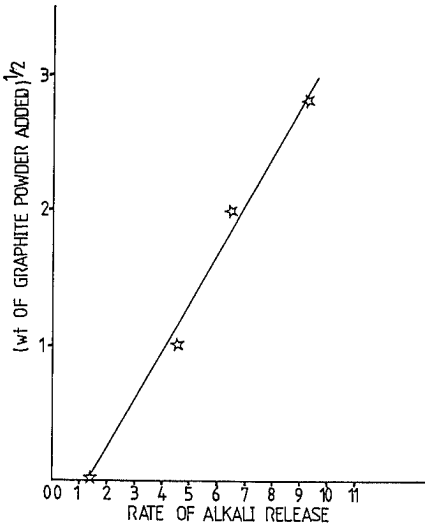

Fig. 12. Effect of graphite addition on rate of Na_2O release from $CaO–Al_2O_3–SiO_2$ slags (INITIAL SLOPES OF FIGURE 50).

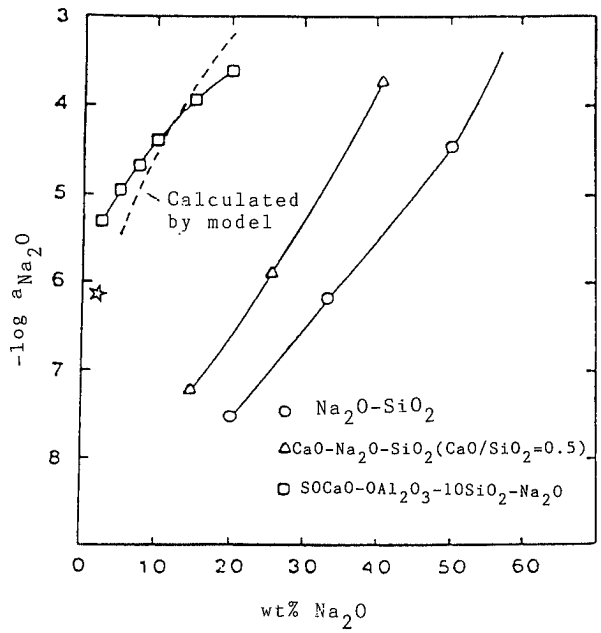

Fig. 13. Comparison of estimated value of Na_2O from present data with data of Pak and Fruehan.
— Present study where:
CaO=27.5
Al_2O_3=32.4
SiO_2=40.1

proportional to the weight of graphite powder added it follows that

$$k_m \propto (\text{wt\% graphite})^{1/2}$$

and hence alkali release rate $\propto$(wt% graphite)$^{1/2}$.

Figure 12 shows the stage 1 slopes for alkali release plotted as a function of the square weight of graphite powder added lending support to the view that liquid phase mass transfer control is controlling stage 1 kinetics.

Stage 1 control would be expected to cease once gas generation and associated stirring ceases. The onset of stage 2 appears to occur at a composition of around 1.5% of Na_2O for the slag studied regardless of the

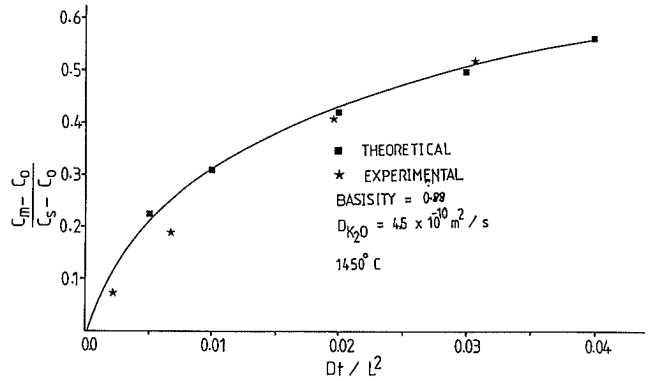

Fig. 14. Comparison of estimated rate of alkali oxide from $CaO–Al_2O_3–SiO_2$ slags and that predicted assuming diffusion control.

Table 5. Effective diffusion coefficients for release rated data.

Slag	Basicity	T (°C)	Initial % Na_2O	D_{Na_2O} ($m^2 s^{-1}$)
V	0.69	1450	4	5×10^{-11}
X	0.88	1450	4	2.6×10^{-10}
F	0.92	1450	7	1.5×10^{-10}
A	0.51	1450	7	0×10^{-11}
B	0.59	1450	7	9×10^{-11}
C	0.79	1450	7	1.2×10^{-10}
D	0.71	1450	7	1.2×10^{-10}
E	0.88	1450	7	4.5×10^{-10}
F	0.92	1450	7	5.5×10^{-10}
G	0.98	1450	7	8.0×10^{-10}
A	0.51	1450	4	7.2×10^{-11}
M	0.64	1450	4	1×10^{-10}
E	0.88	1450	4	5.5×10^{-10}

weight of graphite added to the slag. Gas generation occurs by

$$Na_2O + C \longrightarrow 2Na + CO\,.$$

Assuming that gas generation ceases when $p_{Na}+p_{CO}=$ 1 atm the activity of Na_2O in the slag $a_{Na_2O(l)}$ can be estimated to be 8×10^{-7} in a slag of composition 1.5% Na_2O in 27.5% CaO, 32.4% Al_2O_3, 40.1% SiO_2 at 1450°C. This estimate is compared with the data of Pak and Fruehan[26] for Na_2O activities in slags in **Fig. 13.**

The observed rate data for stage 2 can be analysed by assuming that they correspond to diffusion of alkali oxide to the slag/gas interface. As in the previous analysis of binary system data it is appropriate to consider diffusion to the surface of a hemisphere of the same radius as the graphite crucible. **Figure 14** shows an example of the type of fit obtained by judicious choice of diffusion coefficient (D). **Table 5** summarises values of D that were found to give good agreement with experimental data and provides comparison with literature values for interdiffusion coefficients.

Observation of the slag shape in the crucible indicated that the onset of stage 3 kinetics was associated with a change from the slag not wetting the crucible to the slag wetting the crucible. The conditions under which this change of mechanism occurred were found to be

- high temperature: wetting was usually observed at 1 650°C but only with long reaction times and in slags of low basicity at 1 450°C;
- argon atmosphere, in contrast to CO atmosphere which favoured non-wetting;
- slags containing K_2O appeared to show wetting at an earlier stage of the reduction experiment than slags containing Na_2O.

These observations are consistent with the formation of silicon carbide as an interface product between the slag and the graphite being responsible for the onset of wetting.

At 1 650°C thermodynamic calculations indicate that SiC formation would be expected to occur readily, leading to the generation of CO pressures greater than 1 atm. Such CO generation may result in stirring of the slag and thus be responsible for the observed enhancement of reaction kinetics in stage 3. Such an explanation is unlikely, however, during reduction at 1 450°C.

The change to wetting of the crucible by the slag produces a change in geometry which produces an overall shorter diffusion path to the slag/gas interface and thus would be anticipated to produce an associated increase in reaction kinetics. Analysis of rate data assuming diffusion to the surface of a half slab shows reasonable agreement between theoretical prediction and experimental data.

It is clear that the presence of K_2O in the slag catalyses the reaction of carbon to yield SiC to a greater extent than does Na_2O. This is in agreement with known catalytic effects of both of these species on the reactions of carbon.

Additions of S to slags were found to decrease reaction kinetics whereas additions of iron were found to inverse reaction kinetics. These effects have been attributed to the effects of S and Fe on the wetting of graphite by slags and associated changes in the diffusion paths to the slag/gas interface.

6. Conclusions

Our recent work at Imperial College has highlighted the importance of several interfacial phenomena in controlling the dispersion of reaction products and the kinetics of reactions.

Of particular note are our observations highlighting:

- the apparent role of associative adsorption phenomena in altering interfacial properties and thus permitting dispersion of phases under unexpected conditions;
- the role of the formation of interfacial products in altering interfacial properties and thus permitting dispersion of phases;
- anomalous decreases in interfacial tension during the course of reactions apparently not capable of being explained by the role of intense mass transfer during the reaction;
- the role of gas bubble generation at interfaces in promoting bulk stirring of phases and enhancement of reaction kinetics;
- the role of the formation of interfacial products in altering interfacial properties and in thus altering geometrical configurations of reactants with resultant changes in diffusion paths and reaction kinetics.

Such phenomena undoubtedly operate in many other systems and situations of industrial relevance. Their identification and control can only serve to assist the improvement and development of materials processing routes.

REFERENCES

1) K. S. Coley, B. S. Terry and P. Grieveson: Terkel Rosenquist Symp., ed. by S. E. Olsen and J. K. Tvset, Trondheim, May, (1988).
2) K. S. Coley: Ph.D. Thesis, Imperial College, London, (1986).
3) D. J. O'Brien and D. Gain: *N.Z. J. Science*, **10** (1967), 736.
4) D. J. O'Brien and T. Marshall: *N.Z. J. Science*, **8** (1965), 3.
5) D. J. O'Brien and T. Marshall: *N.Z. J. Science*, **11** (1968), 159.
6) S. S. Kiparisov: *Sov. Powder Metall. Met. Ceram.*, **15** (1976), No. 8, 618.
7) S. S. Kiparisov: *Sov. Powder Metall. Met. Ceram.*, **15** (1976), No. 6, 618.
8) T. J. Whalen: *Trans. Am. Soc. Met.*, **55** (1962), 778.
9) G. R. Belton: *Metall. Trans.*, **3** (1972), 465.
10) B. S. Terry and O. S. Chinyamakobvu: *Mater. Sci. Technol.*, (1991), No. 6.
11) B. S. terry and O. S. Chinyamakobvu: *Mater. Sci. Technol.*, (1992), No. 5.
12) B. S. Terry and O. S. Chinyamakobvu: *J. Mater. Sci.*, in press.
13) B. S. Terry and O. S. Chinyamakobvu: *J. Mater. Sci.*, in press.
14) B. S. Terry and O. S. Chinyamakobvu: *Mater. Sci. Technol.*, (1992), No. 6.
15) J. Ellis: Ph.D. Thesis, Imperial College, London, (1992).
16) M. S. Lee, B. S. Terry and P. Grieveson: *Met. Trans. B*, in press.
17) M. S. Lee, B. S. Terry and P. Grieveson: *Met. Trans. B*, in press.
18) P. V. Riboud and L. D. Lucas: *Can. Metall. Q.*, **20** (1981), 199.
19) G. R. Asjadi: Ph.D. Thesis, Imperial College, London, (1992).
20) B. S. Terry and G. R. Asjadi: *Glass Technology*, submitted for publication.
21) B. S. Terry and G. R. Asjadi: *Ironmaking Steelmaking*, submitted for publication.
22) B. S. Terry and G. R. Asjadi: *Ironmaking Steelmaking*, submitted for publication.
23) J. M. Steiler: Physicochimie et Siderugie, Versailles, Oct., (1978).
24) D. Rego, G. K. Sigworth and W. O. Philbrook: *Metall. Trans. B*, **16B** (1985), 313.
25) B. Staples, D. Robertson and F. D. Richardson: Darken Conf., US Steel Corp., (1976).
26) J. Pak and R. J. Fruehan: 3rd Int. Conf. in Molten Slags and Fluxes, Strathclyde, (1988).
27) H. B. May and R. Wollast: *J. Am. Ceram. Soc.*, **57** (1974), 30.
28) K. Schwerdtfezer: *J. Phys. Chem.*, **70** (1966), 2131.